COMPDYN 2013
4th ECCOMAS Thematic Conference on
Computational Methods in Structural Dynamics and Earthquake Engineering
M. Papadrakakis, V. Papadopoulos, V. Plevris (eds.)
Kos Island, Greece, 12–14 June 2013

IDENTIFICATION OF REINFORCED CONCRETE BEAM PARAMETERS USING INVERSE MODELING TECHNIQUE AND MEASURED DYNAMIC RESPONSES FOR STRUCTURE HEALTH MONITORING

J. Waeytens[1], V. le Corvec[2], P. Lévèque[1], D. Siegert[1] and F. Bourquin[1]

[1]Université Paris-Est, IFSTTAR
boulevard Newton, F-77747 Champs sur Marne, France
e-mail: {julien.waeytens,philippe.leveque,dominique.siegert,frederic.bourquin}@ifsttar.fr

[2] Numerical Engineering & Consulting Services
196, rue Houdan, F-F-92330 Sceaux, France
e-mail: veronique.lecorvec@necs.fr

Keywords: Inverse problem, optimal control, adjoint problem, structural dynamics.

Abstract. *Reinforced and prestressed concrete beams are widely employed in civil engineering structures, e.g. in simply supported spans using prestressed concrete beams (VIPP). To reduce the financial cost due to maintenance, structure damages have to be detected early. To achieve this purpose, one needs robust monitoring techniques.*
The paper deals with the determination of mechanical parameters, useful for Structure Health Monitoring, in a 2D beam using inverse modeling technique. The optimal control theory is employed. As an example, we aim to identify a reduction of the steel bar cross-section and a decrease of the concrete Young modulus in damaged area. In our strategy, the beam is instrumented with strain sensors, and a known dynamic load is applied. In the inverse technique, two space discretizations are considered: a fine dicretization (h) to solve the structural dynamic problem and a coarse discretization (H) for the beam parameter identification. To get the beam parameters, we minimize a classical data misfit functional using a gradient-like algorithm. A low-cost computation of the functional gradient is performed using the adjoint problem solution. The inverse problem is solved in a general way using engineer numerical tools: Python scripts and the free finite element software Code_Aster. First results show that a local reduction of the steel bar cross-sections and a local decrease of concrete Young modulus can be detected using this inverse technique.

1 INTRODUCTION

Prestressed and reinforced beams are widely employed in civil engineering structures. Between 1945 and 1965, 1000 prestressed concrete bridges were constructed, 550 were of the VIPP type (independent span viaducts with prestressed beams) [1]. Thus, the maintenance of such structures is a central issue. To reduce maintenance costs, the damaged beams in the structure have to be identified early. To achieve this purpose, the beams should be monitored and non-destructive control methods should be used. Inverse techniques using dynamic responses have been developed in [2] to identify the prestress force in a beam. A one-dimensional (1D) beam modelisation was considered. In the present article, we focus on inverse problems based on two-dimensional (2D) beam modelisation. As a matter of fact, by means of 2D modelisation, we can specify the 2D position of the sensors and we can precisely describe the geometry and the position of steel bars. Using dynamic strain responses, we are interested in identifying a local loss of steel bar cross-section and a local decrease of concrete Young modulus. For that, an inverse modeling technique based on the optimal control theory [3] is proposed. In the 2D elastodynamics direct problem, the dynamic loading is considered known. The inverse problem is solved in a general way using common engineering numerical tools: free finite element software Code_Aster [4], Python Numpy library and a Python mesh API provided by SALOME platform [5]. On a 2D concrete beam with a single steel bar, we show that a 25% local loss of the steel bar cross-section and a 25% local decrease of the concrete Young modulus can be detected with the proposed method.
The article is organized as follows: in Section 2, the inverse method is presented; in Section 3, details about the numerical implementation are given and in Section 4, the inverse method is illustrated on a 2D concrete beam with a steel bar.

2 METHODOLOGY TO IDENTIFY A REDUCTION OF THE STEEL BAR CROSS-SECTIONS AND A LOCAL DECREASE OF THE CONCRETE YOUNG MODULUS IN A 2D CONCRETE BEAM

We aim at identifying the steel bar cross-section $S_b(\underline{x})$ and the concrete Young modulus $E_c(\underline{x})$ in a 2D concrete beam from the knowledge of measured strain. Note that the dynamic loading applied to the concrete beam is considered known. To determine the beam mechanical parameters, an inverse modeling technique is employed. As usual in the optimal control theory, we seek the steel bar cross-section $S_b(\underline{x})$ and the concrete Young modulus $E_c(\underline{x})$ such that it minimizes a data misfit functional. The minimization process is performed in an iterative way using the steepest descent direction (gradient method). At each iteration, the main steps are the followings:

- solve the direct problem (elastodynamics equations forward in time) considering the beam parameters $S_b(\underline{x})$ and $E_c(\underline{x})$ of the previous iteration;
- solve the adjoint problem (elastodynamics equations backward in time);
- compute the functional gradient using the direct and the adjoint states;
- update the steel bar cross-section $S_b(\underline{x})$ and the concrete Young modulus $E_c(\underline{x})$.

2.1 Beam parameters to be determined

To reduce the number of beam parameters to be identified, $S_b(\underline{x})$ and $E_c(\underline{x})$ are sought under the form:

$$S_b(\underline{x}) = \sum_{j=1}^{n_b} \bar{S}_{bj} S_{b_{ud}}\, \phi_j^s(x),\ E_c(\underline{x}) = \sum_{j=1}^{n_c} \bar{E}_{cj} E_{c_{ud}}\, \phi_j^c(x) \tag{1}$$

where:

- $S_{b_{ud}}$ (resp. $E_{c_{ud}}$) corresponds to the undamaged cross-section of the steel (resp. the undamaged Young modulus of the concrete);
- $\bar{S}_{bj}$ (resp. $\bar{E}_{cj}$) represents the j^{th} normalized cross-section of the steel (resp. normalized Young modulus of the concrete) associated to the area Γ_j (resp. Ω_{c_j}), *i.e.* the area where $\phi_j^b(x)$ (resp. $\phi_j^c(x)$) is non-zero. $\bar{S}_{bj}$ and $\bar{E}_{cj}$ have to be determined using the inverse modeling technique;
- $\phi_j^b(x)$ and $\phi_j^c(x)$ are basis functions on a coarse grid mesh (H). They are *a priori* known. In practice, $\phi_j^b(x)$ (resp. $\phi_j^c(x)$) is a constant basis function equal to 1 in the area Γ_j (resp. in the subdomain Ω_{c_j}) and equal to 0 elsewhere.

2.2 Direct problem

In the present study, the shear work and the bending work in the steel bar are neglected. We also neglect the quantity of acceleration in rotation in the steel bar. We suppose that the steel bar and the concrete are perfectly adherent.
We seek the displacement field $\underline{u} \in \mathcal{U}_0 = \{\underline{u}^* \in H_1(\Omega) \backslash \underline{u}^* = \underline{0} \text{ on } \partial\Omega_i\}$ such that :

$$\begin{aligned} &\int_\Omega \rho_c \ddot{\underline{u}}.\underline{u}^* d\Omega + \int_\Gamma \rho_b S_b \ddot{\underline{u}}.\underline{u}^* d\Gamma + \int_\Omega \underline{\underline{\epsilon}}(\underline{u}) : \mathcal{K}_c \underline{\underline{\epsilon}}(\underline{u}^*) d\Omega + \int_\Gamma E_b S_b \frac{\partial u_x}{\partial x}\frac{\partial u_x^*}{\partial x} d\Gamma \\ &- \int_{\partial\Omega_f} \underline{F}_d.\underline{u}^* \partial\Omega = 0,\ \forall \underline{u}^* \in \mathcal{U}_0 \end{aligned} \tag{2}$$

The initial conditions are supposed to vanish.

2.3 Data misfit functional

We seek the normalized steel bar cross-section $\bar{S}_{bj}$ ($j \in \{1, .., n_b\}$) and the normalized concrete Young modulus $\bar{E}_{cj}$ ($j \in \{1, .., n_c\}$), minimizing the data misfit functional defined as:

$$\begin{aligned} J(\bar{S}_b, \bar{E}_c) = \frac{1}{2}\sum_{i=1}^{n_s} \int_0^T \left[\int_\Omega \epsilon_{xx}(x,t)\psi_i(\underline{x} - \underline{x}_i) d\Omega - (\epsilon_{xx}^{mes})_i(t)\right]^2 dt \quad &+\epsilon_1 \frac{\alpha_{n_1}}{2} \int_\Gamma \left[\frac{S_b(x)}{S_{b_{ud}}} - 1\right]^2 d\Gamma \\ &+\epsilon_2 \frac{\alpha_{n_2}}{2} \int_\Omega \left[\frac{E_c(x)}{E_{c_{ud}}} - 1\right]^2 d\Omega \end{aligned} \tag{3}$$

where:

- n_s is the number of strain sensors;

- $(\epsilon_{xx}^{mes})_i(t)$ is xx strain measured by sensor i located at $\underline{x}_i$;
- $\psi_i(\underline{x}-\underline{x}_i)$ is the spatial weight function associated to sensor i.

In (3), one has a classical quadratic data misfit term and regularization terms. ϵ_1 and ϵ_2 are normalized regularization parameters. α_{n_1} and α_{n_2} ensure the physical homogeneity of the terms in the functional J. Herein, we take:

$$\alpha_{n_1}=\frac{T}{L},\ \ \alpha_{n_2}=\frac{T}{L^2} \tag{4}$$

2.4 Adjoint problem, functional gradient and beam parameter update

To get the functional gradient at a low computational cost, we use the adjoint state. In this study, the adjoint problem corresponds to a backward elastodynamics problem (final conditions vanish).
We seek the displacement $\tilde{\underline{u}} \in \mathcal{U}_0=\{\underline{u}^* \in H_1(\Omega)\backslash \underline{u}^*=\underline{0} \text{ on } \partial\Omega_i\}$ satisfying:

$$\begin{aligned}&\int_\Omega \rho_c \ddot{\tilde{\underline{u}}}.\underline{u}^* d\Omega+\int_\Gamma \rho_b S_b \ddot{\tilde{\underline{u}}}.\underline{u}^* d\Gamma+\int_\Omega \underline{\underline{\epsilon}}(\tilde{\underline{u}}):\mathcal{K}_c\underline{\underline{\epsilon}}(\underline{u}^*)d\Omega+\int_\Gamma E_b S_b \frac{\partial \tilde{u}_x}{\partial x}\frac{\partial u_x^*}{\partial x}d\Gamma\\ &-\sum_{i=1}^{n_s}\int_\Omega\left[\int_\Omega \epsilon_{xx}(\underline{x},t)\psi(\underline{x}-\underline{x}_i)d\Omega-(\epsilon_{xx}^{mes})_i(t)\right]\psi_i(\underline{x}-\underline{x}_i)\frac{\partial u_x^*}{\partial x}d\Omega dt=0,\ \forall \underline{u}^*\in\mathcal{U}_0\end{aligned} \tag{5}$$

Note that this problem can be solved using classical finite element codes.

From the direct and the adjoint states, we obtain the gradient of the functional, as follows:

$$\begin{aligned}\frac{\partial J}{\partial \bar{S}_{bj}}=&-\int_0^T\int_\Gamma E_b S_{b_{ud}}\phi_j^b(x)\frac{\partial u_x}{\partial x}\frac{\partial \tilde{u}_x}{\partial x}d\Gamma dt-\int_0^T\int_\Gamma \rho_b S_{b_{ud}}\phi_j^b(x)\ddot{\underline{u}}.\tilde{\underline{u}}d\Gamma dt\\ &+\epsilon_1\alpha_{n_1}\int_\Gamma\left(\frac{S_b(x)}{S_{b_{ud}}}-1\right)\phi_j^b(x)d\Gamma\end{aligned} \tag{6}$$

$$\begin{aligned}\frac{\partial J}{\partial \bar{E}_{cj}}=&-\int_0^T\int_\Omega d\lambda_{DP}\phi_j^c(x)div(\underline{u})div(\tilde{\underline{u}})d\Omega dt-\int_0^T\int_\Omega 2d\mu_{DP}\phi_j^c(x)\underline{\underline{\epsilon}}(\underline{u}):\underline{\underline{\epsilon}}(\tilde{\underline{u}})d\Omega dt\\ &+\epsilon_2\alpha_{n_2}\int_\Omega\left(\frac{E_c(x)}{E_{c_{ud}}}-1\right)\phi_j^c(x)d\Omega\end{aligned} \tag{7}$$

where:

$$d\lambda_{DP}=\frac{E_{c_{ud}}\nu_c}{(1+\nu_c)(1-\nu_c)},\ d\mu_{DP}=\frac{E_{c_{ud}}}{2(1+\nu_c)} \tag{8}$$

Once we get the functional gradient, several solves of the direct problem are performed to determine the optimal descent step and we deduce the new set of beam parameters.

3 NUMERICAL IMPLEMENTATION

The inverse problem is solved in a general way using state of the art finite element softwares. A synthesis of the numerical steps is given in Figure 3. From a main Python script, we run the finite element software Code_Aster to solve the direct and adjoint problems, which are elastodynamics problems. We specify to Code_Aster Python supervisor to serialize, thanks to Python

pickle module, the fields useful for the gradient computation and to export the strain $(\epsilon_{xx}^{sim})_i$ computed at the sensor location $\underline{x}_i$. Note that the loading of the adjoint problem corresponds to a 'xx' internal stress $(\tilde{\sigma}_{0_{xx}})_i$ in the vicinity of the i^{th} sensor location. This loading (see (5)) is given by the data misfit δ:

$$(\tilde{\sigma}_{0_{xx}})_i(\underline{x},t) = \left[(\epsilon_{xx}^{sim})_i(t) - (\epsilon_{xx}^{mes})_i(t)\right] \psi_i(\underline{x}-\underline{x}_i),\ i \in \{1,..,n_s\} \tag{9}$$

In practice in Code_Aster, the spatial weight function $\psi_i(\underline{x}-\underline{x}_i)$ is constant in the patch of elements associated to the i^{th} sensor node. To compute the gradient of the data misfit functional according to the formulas (6,7), for the direct problem, one needs the acceleration $\underline{\ddot{u}}$ in the steel bar and the strain $\underline{\underline{\epsilon}}$ in the steel and the concrete parts. Concerning the adjoint problem, one needs the displacement $\underline{\tilde{u}}$ in the steel bar and the strain $\underline{\underline{\tilde{\epsilon}}}$ in the beam. Using these fields and mesh data, the gradient is computed from a python script. Then, to determine the optimal descent step, which minimizes the data misfit functional, several resolutions of the direct problem are performed using Code_Aster. Once the optimal descent step is obtained, we deduce the new set of beam parameters. The iterative process stops when the data misfit δ is about the sensor precision.

4 NUMERICAL EXAMPLE

4.1 Definition of the identification problem

A 2D concrete beam with a single horizontal steel bar is considered (see Figure 2). Plane strain is assumed. A dynamic load is applied to the top of the concrete beam, it is defined as:

$$\underline{F}_d(t) = \begin{cases} -F_{max} sin\left(\dfrac{2\pi}{T_c}t\right)\underline{y},\ t \in [0, T_c/2[\\ 0,\ t \in [T_c/2, T] \end{cases} \tag{10}$$

Numerical values: $F_{max} = 10^4 N/m^2,\ T_c = 2s,\ T = 5s.$

In this study, the steel bar is decomposed into 5 pieces ($n_b = 5$ in (1)). In each piece j, one has a constant steel bar cross-section S_{b_j}. Concerning the concrete zone, we only consider a loss of Young modulus in the concrete part named Ω_c which is under the steel bar. In the same way, the domain Ω_c is decomposed into 5 subdomains ($n_c = 5$ in (1)). In each concrete subdomain j, a constant Young modulus E_{c_j} is taken. We assume that the steel bar cross-section (resp. the concrete Young modulus) is known and undamaged in pieces 1 and 5 (resp. in subdomains 1 and 5): $S_{b_1} = S_{b_5} = S_{b_{ud}}$ (resp. $E_{c_1} = E_{c_5} = E_{c_{ud}}$). As a result, we aim at identifying by the inverse modeling technique the normalized steel bar cross-sections and the normalized concrete Young modulus $\bar{S}_{b2}, \bar{S}_{b3}, \bar{S}_{b4}, \bar{E}_{c2}, \bar{E}_{c3}, \bar{E}_{c4}$ defined as:

$$S_{b_j} = \bar{S}_{bj} S_{b_{ud}},\ \text{with } S_{b_{ud}} = 0,04; \quad E_{c_j} = \bar{E}_{cj} E_{c_{ud}},\ \text{with } E_{c_{ud}} = 40\ GPa \tag{11}$$

To avoid "inverse crime", we take as reference the numerical solution obtained with the finite element code Freefem++ [6] considering the loading (10) and the beam parameters:

$$\begin{cases} S_{b_1}^{ex} = S_{b_2}^{ex} = S_{b_4}^{ex} = S_{b_5}^{ex} = 0,04\ \& S_{b_3}^{ex} = 0,03 \\ E_{c_1}^{ex} = E_{c_2}^{ex} = E_{c_4}^{ex} = E_{c_5}^{ex} = 40\ GPa\ \& E_{c_3}^{ex} = 30\ GPa \end{cases} \tag{12}$$

To solve the elastodynamics problem, we take the inconditionally stable Newmark scheme ($\gamma = 1/2, \beta = 1/4$). In practice, the data outputs ϵ_{xx}^{mes} are measured. Nevertheless, herein, ϵ_{xx}^{mes} is

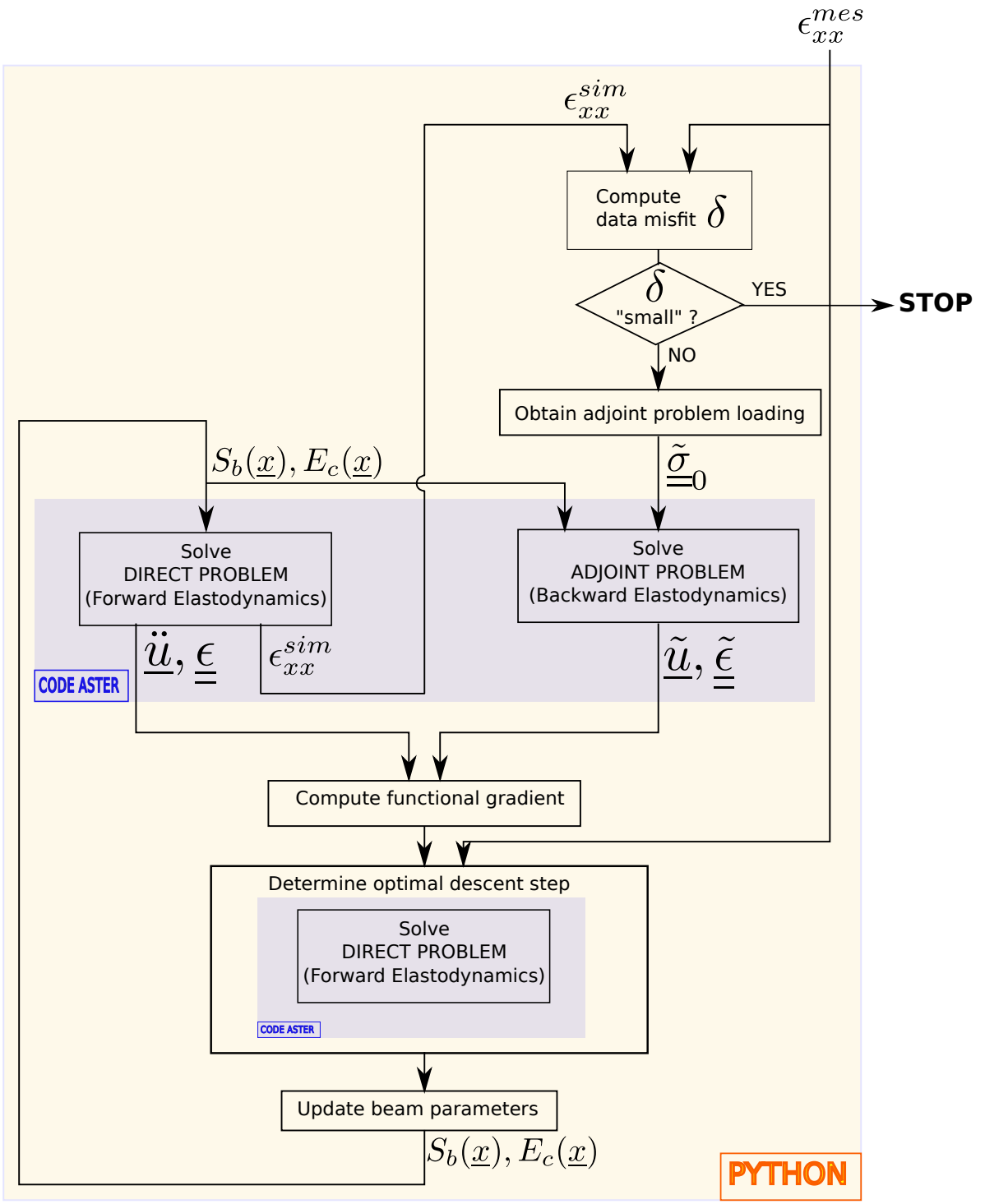

Figure 1: Methodology for beam parameter identification

deduced from the reference numerical solution. We consider 7 strain sensors in the concrete beam, there are located at:

$$S_1 : (3L/16, H/8); S_2 : (5L/16, H/8); S_3(7L/16, H/8); S_4(L/2, H/8); S_5(9L/16, H/8); \\ S_6 : (11L/16, H/8); S_7(13L/16, H/8). \tag{13}$$

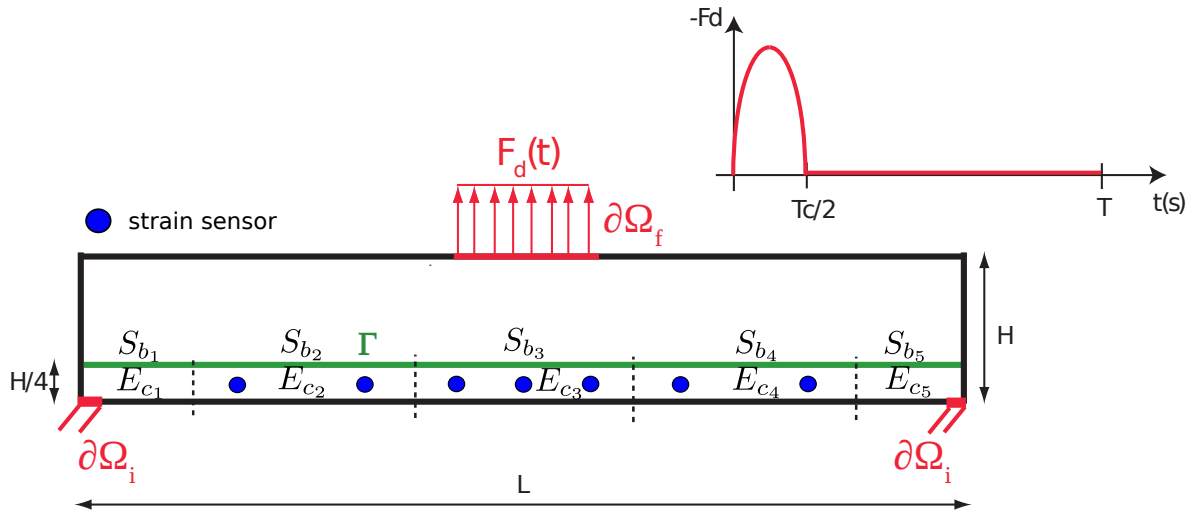

Figure 2: Concrete beam with a horizontal steel bar - Steel bar decomposed in 5 pieces. Each piece has a constant cross-section - Lower Concrete part decomposed in 5 subdomains. Each subdomain has a constant Young modulus - Beam instrumented with 7 strains sensors.

	k	δ_k	$e_k^{rel}(\%)$	S_{b_2}	S_{b_3}	S_{b_4}	$E_{c_2}(GPa)$	$E_{c_3}(GPa)$	$E_{c_4}(GPa)$
it 0	4	$2.9.10^{-7}$	10.3	0.040	0.040	0.040	40.0	40.0	40.0
it 1	2	$1.7.10^{-7}$	36.0	0.040	0.040	0.040	39.6	35.2	39.4
it 2	2	$1.6.10^{-7}$	33.7	0.040	0.039	0.040	40.0	34.1	39.4
it 3	2	$1.4.10^{-7}$	28.3	0.039	0.035	0.039	40.0	31.7	40.0
it 4	2	$1.4.10^{-7}$	28.0	0.040	0.035	0.039	40.0	31.5	40.0

Table 1: Steel bar cross-sections and Concrete Young modulus at each iteration of the inverse modeling technique

4.1.1 Solution of the inverse modeling technique

The results of the beam identification are given at each iteration of the inverse modeling technique in Table 1. At each iteration of the inverse technique, we evaluate the data misfit δ and its relative error e^{rel} defined by:

$$\begin{cases} \delta_i = \left(\int_0^T \left[(\epsilon_{xx}^{sim})_i(t) - (\epsilon_{xx}^{mes})_i(t) \right]^2 dt \right)^{1/2}, \ i \in \{1, .., n_s\} \\ e_i^{rel} = \dfrac{\delta_i}{\left(\int_0^T \left[((\epsilon_{xx}^{mes})_i(t) \right]^2 dt \right)^{1/2}}, \ i \in \{1, .., n_s\} \end{cases} \tag{14}$$

In Table 1, the value of the maximum data misfit and its associated relative error are given, k corresponds to the sensor number which has the highest data misfit.

We underline the fact that these results are obtained considering "small" regularization parameters ($\epsilon_1 = 10^{-16}, \epsilon_2 = 10^{-13}$). After the third iteration, we note that the data misfit reaches a plateau. It corresponds to the error between a numerical solution obtained with FreeFem++ and a numerical solution computed with Code_Aster. As a consequence, the inverse technique should be stopped at iteration 4. At iteration 4, one has a 28% error between the 'xx' strain

measured at sensor 2 and the reconstructed strain. This leads to a 5% error on the identification of the concrete Young modulus in subdomains 3 and to a 15% error on the identification of the steel bar cross-section in piece 3. We recall that the reference values of concrete Young modulus and steel bar cross-sections are given in (12).

5 CONCLUSIONS

To identify the beam parameters (steel bar cross-sections and concrete Young modulus), we proposed an inverse modeling technique based on 2D elastodynamics model and dynamic strain responses. On the 2D concrete beam with a single steel bar, we showed that a 25% local loss of the steel bar cross-section and a 25% local decrease of the concrete Young modulus could be detected. In forthcoming papers, real data outputs will be considered and more representative 2D beam models [7, 8] will be employed in the inverse technique.

6 ACKNOWLEDGMENTS

This research was supported by the region Ile de France. This work was conducted as part of the project "SIPRIS", which involves several partner: Advitam (leader), ASF (Highways of the South of France), CEDRAT, ESIEE Paris, NECS, NEWSTEO, SYROKKO and IFSTTAR.

REFERENCES

[1] J. Chatelain, R. Chaussin, B. Godart, B. Mahut, D. Poineau, P. C. Das, G. A. Paterson, B. Sadka, S. Shanmugan, D. B. Storrar, R. J. Woodward, *Post-tensioned concrete bridges*. Thomas Telford, 1999.

[2] Z.R. Lu, S. S. Law, Identification of prestress force from measured structural responses. *Mechanical Systems and Signal Processing*, **20**, 2186–2199, 2006.

[3] J.L. Lions, *Contrôle Optimal des Systèmes Gouvernés par des Equations aux Dérivées Partielles*. Dunod (Paris), 1961 (in french).

[4] Code_Aster, EDF R& D, Finite element code for structural analysis, GNU general public licence, *http://www.code-aster.org*.

[5] Salome, CEA/DEN, EDF R& D, OPEN CASCADE, Open Source Integration Platform for Numerical Simulation, *http://www.salome-platform.org*.

[6] O. Pironneau, F. Hecht, J. Morice, FreeFEM++, *http://www.freefem.org*.

[7] A. Castel, D. Coronelli, N. A. Vu, R. Francois, Structural response of Corroded, Unbonded Posttensioned Beams. *Structural Engineering*, **137**, 7, 761–771, 2011.

[8] A. A. Arab, S. S. Badie, M. T. Manzari, A methodological approach for finite element modeling of pretensioned concrete members at the release of pretensioning. *Engineering Structures*, **33**, 1918–1929, 2011.